

# Chapter 2

## Some Industrial Systems

### 2.1 Introduction

Identification of process parameters for control purposes must often be done using a digital computer, from samples of input–output observations. On the other hand, the process is usually of continuous-time nature, and its dynamical model is most aptly described in terms of differential equations. Thus, our problem may be stated as determining a continuous-time model from samples of input–output data.

During the past few decades, several approaches have been developed [30, 46–48]. For the sake of simplicity, these can be classified as

- direct methods,
- indirect methods.

Methods belonging to the first type attempt to estimate the parameters of a continuous-time model directly from the samples of the observations, mostly using some type of numerical integration. In methods of the latter group, the problem is conveniently divided into two subproblems:

The first subproblem consists of estimating the parameters of a discrete-time model from the samples of the input–output observations.

The second subproblem, on the other hand, consists of determining a suitable continuous-time model that is equivalent to the discrete-time model obtained for a given sampling interval.

Generally speaking, the problem of system identification may now be stated as the estimation of the elements of the matrices  $A$ ,  $B$ ,  $C$ ,  $D$  associated with the linear time-invariant system

$$\begin{aligned}\dot{x}(t) &= Ax(t) + Bu(t), \\ y(t) &= Cx(t) + Du(t)\end{aligned}\tag{2.1}$$

from a record of the samples of the input output data

$$\{u(kT), y(kT)\}, \quad \text{for } k = 0; 1; 2; \dots; N$$

where  $N$  is a suitable large number.

It may be noted that the matrix  $D$  represents direct coupling between the input and the output, and will be zero for strictly proper transfer functions. Without any loss of generality and unless otherwise stated, this will be assumed to be the case throughout this book. It should be noted that none of the matrices  $A$ ,  $B$ ,  $C$  in (2.1) are unique for a system with a given input–output description. Given a special canonical form for the system state equations in either the continuous-time or the equivalent discrete time models overcomes this problem and also minimizes the number of parameters to be estimated. It should also be noted that it is tacitly assumed that the order of the linear state space model is known, and that the sampling interval has been suitably selected. In practice, both of these are important, and have been subjects of considerable research [24, 25, 48].

In fact, the problem is further complicated by the fact that the available data are usually contaminated with random noise that are produced either by disturbances or introduced in data acquisition and measurement. The literature on system identification abounds in papers devoted to methods for estimating the parameters in the presence of noise, see [47] for a detailed list of references.

## 2.2 Steam Generation Unit

There are two types of configurations in the electricity generation using drum boilers and steam turbines:

1. A single boiler is used to generate steam that is directly fed to a single turbine. This configuration is usually referred to as a boiler–turbine unit.
2. A header is used to accommodate all the steam produced from several boilers, and the steam is then distributed to several turbines through the header. The steam can be used to generate electricity as well as other purposes. This configuration is commonly used in industrial utility plants.

Boiler–turbine units are nowadays preferred over header systems, because they can achieve quick response to electricity demands from a power grid or network. It is generally accepted that a boiler–turbine unit is a highly nonlinear and strongly coupled complex system. However, there is no definite quantification of the complexity of a unit. Specifically, how nonlinear is it? Can a linear controller be used to cover the whole operating range? These are fundamental issues in the control system design for a boiler–turbine unit. Without a thorough understanding, modeling and identification of the system, the operating range and performance of a linear controller cannot be guaranteed. Figure 2.1 shows the schematic diagram of the steam generator model.

### 2.2.1 System Dynamics

For the system considered here, the input/output experimental data has been obtained from [20] in which the modeling of a steam generator at Abbot power plant

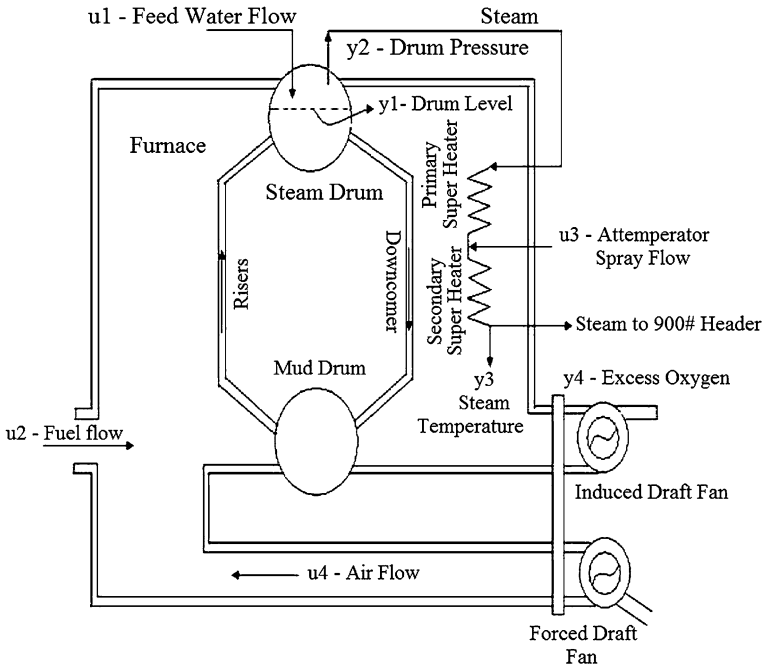


Fig. 2.1 Steam generating unit

in Champaign IL is considered. The data comes from a model of this steam generator. The inputs are listed as follows:

- U1: Fuel scaled 0–1,
- U2: Air scaled 0–1,
- U3: Reference level,
- U4: Disturbance defined by the load level.

The outputs are

- Y1: Drum pressure,
- Y2: Excess oxygen in exhaust gases,
- Y3: Level of oxygen in the drum,
- Y4: Steam flow.

The data values are presented in Fig. 2.2.

The simulation data constitutes 9600 samples at a sampling rate of 3 s, which characterizes a MIMO process. In implementation, a set of 4000 samples (5000 : 9000) are used for testing, another set of 4000 samples (2500 : 6500) for validation purpose. The important statistical parameters of all inputs and outputs are listed in Table 2.1.

time-steps	input fuel	input air	input level ref.	input disturbance	drum pressure	excess oxygen	water level	steam flow
0	0.723567501	0.69162867	-2.283056412	0.017982753	320.0823889	2.506773853	0.0327013	9.302970053
3	0.527147387	0.383020194	-3.716481388	0.01871789	321.7109902	2.545907948	0.284799436	9.662620584
6	0.589603123	0.705814627	-1.530992972	0.020756328	320.9133077	2.360561543	0.203651646	10.99095548
9	0.364854222	0.713277726	-3.173065004	0.022927443	325.0025177	0.027054182	0.326186879	12.43010713
12	0.576540101	0.361978097	-1.796211886	0.020370994	326.6527646	0.285649429	0.753776251	13.68166563
15	0.643106594	0.559504307	-2.80426768	0.023209106	326.1869164	2.631328071	1.851854064	14.60886838
18	0.495364003	0.690460919	-3.207444006	0.016374061	326.5893955	0.997855279	2.302339958	15.71319958
21	0.585075453	0.470516735	-1.041846551	0.015338046	328.734886	0.004474148	2.447356587	16.5363068
24	0.664653688	0.360282868	-1.931675122	0.017923064	329.609686	0.755694209	3.036620233	17.02536888
27	0.643043139	0.574080989	-1.478481089	0.011513461	330.1852705	0.150455487	3.567548546	17.61613049
30	0.464561148	0.387073874	-3.913301903	0.017580064	331.7391065	0.01263697	3.462808629	18.10196376
33	0.404921448	0.660802771	-1.59869963	0.015723326	333.1073413	0.012963788	3.423381121	18.6178379
36	0.724379922	0.446190083	-3.989163444	0.014141722	332.2526813	0.00143049	3.542126862	18.6357234
39	0.731302053	0.697717252	-1.150864528	0.02067146	331.9641902	1.261865971	3.542697727	18.75132224
42	0.716108207	0.470846609	-2.509671086	0.023348293	332.2584412	-0.004533128	3.033217277	19.50889423
45	0.519158864	0.510866342	-0.97339551	0.017045047	332.698191	-0.036224068	2.155174268	20.45663212
48	0.595279473	0.642852826	-3.337995093	0.018983813	333.7106987	-0.028905017	2.130121016	20.89645496
51	0.48403137	0.377171236	-2.516360051	0.010279153	334.9233445	0.032445181	2.267387406	21.02755549
54	0.406252116	0.686653761	-1.666630649	0.020761998	332.9221974	0.066819178	2.219327997	20.83617396
57	0.515172894	0.730148283	-1.756067442	0.01314353	330.9151141	-0.017981385	1.573688265	20.70063463
60	0.353699529	0.487394405	-2.117513651	0.02007896	328.3267396	1.317601729	1.296664701	20.39427621
63	0.51216968	0.64642243	-3.74016714	0.011627354	326.4036469	3.151273589	0.551315927	20.22160655
66	0.453003993	0.718432285	-1.327949705	0.021740968	323.6588589	3.726752428	-0.115948509	19.74100857
69	0.648760825	0.343399712	-2.045945519	0.013691541	322.0601255	3.548648872	-0.543213656	19.84917364
72	0.533849639	0.709241376	-1.831108838	0.012666236	320.4334403	4.010865711	-1.184954324	19.75339354
75	0.399869705	0.348706015	-1.082696127	0.020909792	321.2297867	0.600347579	-1.232502023	19.77856981
78	0.578235907	0.709798053	-1.374318147	0.010350625	319.5896845	0.359864199	-1.678045037	19.79985922
81	0.443618032	0.665604084	-0.861456561	0.022472615	318.0445196	0.5383361	-1.522747247	19.43914125
84	0.63785371	0.535170707	-3.6838049	0.016782261	316.7543457	0.592062835	-1.699705982	19.58416198
87	0.485757786	0.454671747	-1.137821862	0.018268976	314.4978796	2.209165353	-1.99815298	19.49900196
90	0.36006478	0.394841718	-2.856183924	0.012938862	313.3338226	1.636450336	-1.993150363	19.64935081
93	0.66066444	0.704633989	-1.060758232	0.019753636	311.8162066	-0.007715276	-2.187443944	19.32839398
96	0.515891469	0.645825437	-2.579230429	0.013735595	309.1821627	0.087425935	-1.859827468	19.1695092
99	0.612877778	0.356006904	-0.957565452	0.017618584	307.8668511	0.299624857	-2.316410273	19.23562254
102	0.608584721	0.493893118	-2.141022066	0.015179435	309.1451192	0.925039703	-2.456011943	19.27840083
105	0.619788222	0.60421281	-3.952446283	0.014320419	308.4521475	0.020171863	-2.032363803	19.34002846
108	0.369935157	0.695078504	-1.396240297	0.009636202	307.1421935	-0.010024978	-2.204217845	19.34207649
111	0.536819511	0.56283553	-2.278566849	0.020844465	306.7214071	-0.016982704	-2.212139324	19.11273381
114	0.579805316	0.436789359	-3.081064258	0.018543932	304.9138787	1.727690747	-2.153424917	18.86746672
117	0.698441545	0.433841554	-1.304343744	0.017743059	304.230753	2.123490842	-2.020366963	19.07370268
120	0.695132002	0.540081641	-1.354954605	0.010611542	303.2929753	-0.004211119	-2.67449837	19.23870373
123	0.633049299	0.579749551	-3.794079204	0.023729927	303.0388137	-0.024038614	-2.607590229	19.33070714
126	0.666181679	0.713919546	-1.539948697	0.01281085	303.5975859	-0.018974644	-2.552692993	19.74181993
129	0.692100112	0.429825546	-0.853122616	0.010553078	304.0344998	-0.003489681	-2.394882293	19.82902142
132	0.730122251	0.531272784	-1.597177347	0.012054672	305.1232434	0.019294486	-2.115191494	19.73419025

Fig. 2.2 Statistical data pattern

Table 2.1 Statistical data

Input/output	Type	Mean	Standard deviation	Min	Max
$I_1$	Fuel scaled 0–1	0.504	0.229	0.000	1.07
$I_2$	Air scaled 0–1	0.528	0.295	0.000	1.07
$I_3$	Reference level	0.554	2.460	-4.00	4.53
$I_4$	Disturbance	0.004	0.010	-0.015	0.023
$O_1$	Drum pressure	329.4	85.94	154	534
$O_2$	Excess oxygen in air	4.544	6.157	-0.069	21
$O_3$	Drum oxygen level	0.552	2.849	-9.55	12.3
$O_4$	Steam flow	14.85	7.571	1.99	34.6

## 2.3 Small-Power Wind Turbine

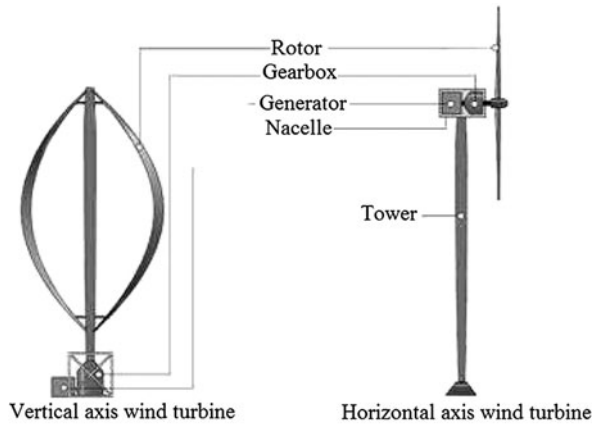
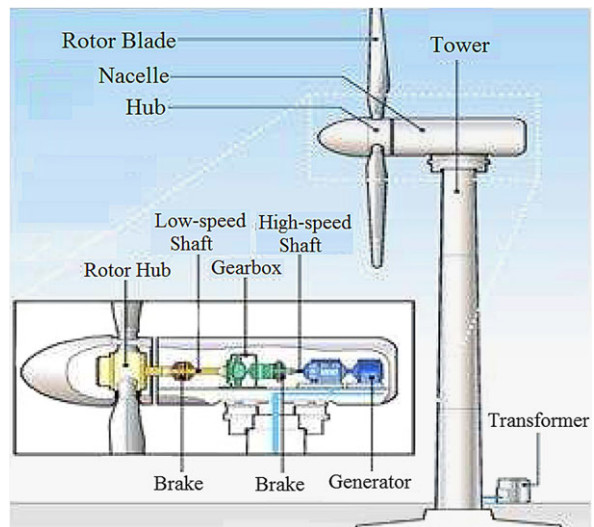
Wind energy is a fast-growing interdisciplinary field that encompasses many different branches of engineering and science. Despite the amazing growth in the installed capacity of wind turbines in recent years, engineering and science challenges still exist. Because larger wind turbines have power capture and economical advantages, the typical size of utility-scale wind turbines has grown dramatically over the last three decades. Modern wind turbines are large, flexible structures operating in uncertain environments and lend themselves nicely to advanced control solutions. Advanced controllers can help achieve the overall goal of decreasing the cost of wind energy by increasing the efficiency, and thus the energy capture, or by reducing structural loading and increasing the lifetimes of the components and turbine structures. In what follows, our goal is to introduce control engineers to the technical challenges that exist in the wind energy industry and to encourage new control systems research in this area.

### 2.3.1 Wind Turbine Basics

The main components of a horizontal-axis wind turbine that are visible from the ground are its tower, nacelle, and rotor. The nacelle houses the generator, which is driven by the high-speed shaft. The high speed shaft is in turn usually driven by a gear box, which steps up the rotational speed from the low-speed shaft. The low-speed shaft is connected to the rotor, which includes the airfoil-shaped blades. These blades capture the kinetic energy in the wind and transforms it into the rotational kinetic energy of the wind turbine. The description of the wind turbine system depends on the designs of the wind turbine either horizontal-axis or vertical axis, see Fig. 2.3.

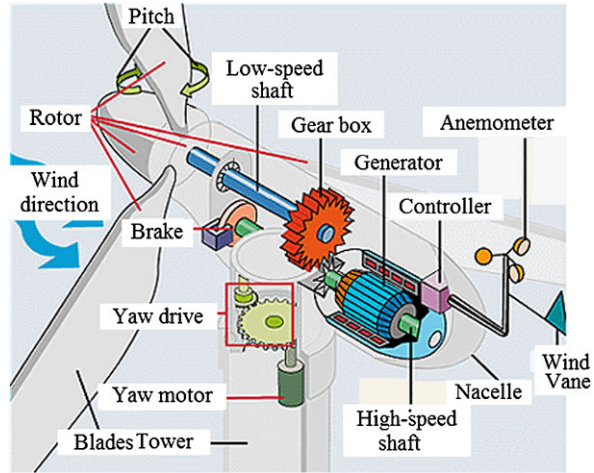
Vertical-axis wind turbines (VAWTs) are pretty rare and the only one currently in commercial production is the Darrieus turbine, which looks kind of like an egg figure. In a VAWT, the shaft is mounted on a vertical axis, perpendicular to the ground. VAWTs are always aligned with the wind, unlike their horizontal-axis counterparts, so there's no adjustment necessary when the wind direction changes. On the other hand, a VAWT is not normally self starting, it needs energy from its electrical system to get started. Instead of a tower, it typically uses wires for support, so the rotor elevation is lower. Lower elevation means slower wind due to ground interference, so VAWTs are generally less efficient than horizontal-axis wind turbines (HAWTs). On the upside, all equipment is at ground level for easy installation and servicing, but that means a larger footprint for the turbine, which is a big negative in farming areas. VAWTs may be used for small-scale turbines and for pumping water in rural areas, but all commercially produced, utility-scale wind turbines are (HAWTs), see Figs. 2.4–2.5.

From its name, the HAWT shaft is mounted horizontally, parallel to the ground. HAWT needs to continuously align itself with the wind speed by using a yaw-adjustment mechanism. The yaw system typically consists of electric motors and

**Fig. 2.3** VAWT and HAWT**Fig. 2.4** The main components of HAWT

gearboxes which move the whole rotor left or right in small increments to hold the higher speed. The turbine's electronic controller reads the position of a wind vane device either mechanical or electronic and adjusts the position of the rotor to capture the most wind energy available [26]. HAWTs use a tower to lift the turbine components to an optimum elevation for wind speed and so the blades can take up very little ground space since wind velocities increase at higher altitudes due to surface aerodynamic drag and the viscosity of the air. Horizontal-axis wind turbines have the main rotor shaft and electrical generator at the top of a tower and must be pointed into the wind. Small turbines are pointed by a simple wind vane, while large turbines generally use a wind sensor coupled with a servo motor. Most of HAWTs have a gearbox which turns the slow rotation of the blades into a quicker rotation that is more appropriate to drive an electrical generator. The main components of

**Fig. 2.5** Parts inside the wind turbine



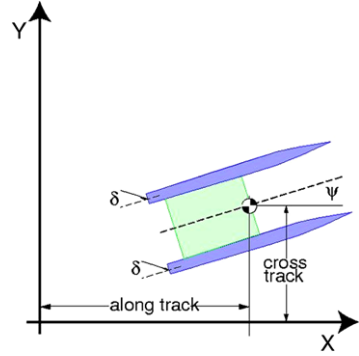
HAWTs are Rotor blades which capture wind's energy and convert it to rotational energy of low speed shaft and Shaft that transfers rotational energy into generator. Also, Nacelle casing that holds Gearbox which increases speed of shaft between rotor hub and generator, Generator that uses rotational energy of shaft to generate electricity using electromagnetism and usually an induction generator that produces AC electricity is used. Moreover, Electronic control unit that monitors system and starts up the machine at wind speeds of about 3–8 m/s and shuts down the machine at about 20 m/s which turbines do not operate at wind speeds above about 20 m/s because they might be damaged by the high winds, Yaw controller is used to keep the rotor facing into the wind as the wind direction changes, and Brakes that stop rotation of shaft in case of power overload or system failure.

In addition to these components, the tower that used to support rotor and nacelle and lifts entire setup to higher elevation where blades can safely clear the ground and towers are made from tubular steel, concrete, or steel lattice. Wind speed increases with height and this mean, taller tower enable turbines to capture more energy and generate more electricity. The electrical equipment that is used to transmit electricity from generator down through tower and controls many safety elements of turbine, and anemometer that measures the wind speed and transmits these readings to the controller. The most commonly activated safety system in a turbine is the braking system, which is triggered by above-threshold wind speeds. These setups use a power-control system that essentially hits the brakes when wind speeds get too high and then release the brakes when the wind is coming back.

## 2.4 Unmanned Surface Marine Vehicle

The Atlantis is assumed to be traveling upon a straight line, conveniently assumed to be coincident with the x-axis, through water at a constant velocity,  $V_x$ . The dis-

**Fig. 2.6** A schematic model of the assumed path of the Atlantis



tance along that line is  $X$  (meters), the perpendicular distance to the line is  $Y$  (meters), the cross-track error, and the angle that the center-line of the Atlantis makes with the  $x$ -axis is  $\Psi$ , the angular error (radians). Figure 2.6 illustrates a schematic model of the assumed path of the Atlantis. The coordinate frame can always be rotated to have the  $x$ -axis aligned to the desired path of the Atlantis, and so the assumption that the Atlantis travels down the  $x$ -axis is a good one. The assumption of constant velocity, however, is not appropriate since velocity is a function of the wind speed. Wind speed, of course, cannot be controlled and is highly variable.

### 2.4.1 Dynamic Model

The continuous-time state-space equations for the kinematic model can be represented as

$$\begin{bmatrix} \dot{Y} \\ \dot{\Psi} \\ \dot{\delta} \end{bmatrix} = \begin{bmatrix} 0 & V_x & 0 \\ 0 & 0 & \frac{V_x}{L} \\ 0 & 0 & 0 \end{bmatrix} \begin{bmatrix} Y \\ \Psi \\ \delta \end{bmatrix} + \begin{bmatrix} 0 \\ 0 \\ 1 \end{bmatrix} u \quad (2.2)$$

where  $\delta$  is the angle of the rudders with respect to the hull center-line (radians). The distance  $L$  is from the boat center of mass to the center of pressure of the rudders (in meters), and the input,  $u$ , is the slew rate of the rudders (in radians/second). This kinematic model assumes that the boat is running on constant  $V_x$ . This assumption is known to be poor, since unless the wind can be controlled, the velocity will always be dependent on the speed of the wind. Azimuth and cross-track error in fact do not integrate with time, but rather with distance traveled upon the line. This has great implications, since this is exactly the cause of instability with increasing velocity present in the simple kinematic model. By introducing two new variable,

$$\tilde{Y} \equiv \frac{Y}{V_x}, \quad \tilde{\Psi} \equiv \frac{\Psi}{V_x}. \quad (2.3)$$

Substituting (2.3) back into (2.2), the kinematic model can be rewritten in the following velocity-invariant form:

$$\begin{bmatrix} \dot{\tilde{Y}} \\ \dot{\tilde{\Psi}} \\ \dot{\delta} \end{bmatrix} = \begin{bmatrix} 0 & 1 & 0 \\ 0 & 0 & \frac{1}{L} \\ 0 & 0 & 0 \end{bmatrix} \begin{bmatrix} \tilde{Y} \\ \tilde{\Psi} \\ \delta \end{bmatrix} + \begin{bmatrix} 0 \\ 0 \\ 1 \end{bmatrix} u. \quad (2.4)$$

## 2.5 Industrial Evaporation Unit

An identification experiment is performed by exciting the system with appropriate signals and observing its input and output over a time interval. These signals are normally recorded in a computer mass storage for subsequent information processing. Then one proceeds to fit a parametric model of the process from the recorded input and output sequences. The first step is to determine an appropriate form of the model (typically a linear difference equation of a certain order). As a second step some statistically based method is used to estimate the unknown parameters of the model (such as the coefficients in the difference equation). In practice, the estimations of structure and parameters are often done iteratively. This means that a tentative structure is chosen and the corresponding parameters are estimated. The model obtained is then tested to see whether it is an appropriate representation of the system. If this is not the case, some more complex model structure must be considered, its parameters estimated, the new model validated, etc. Note that the ‘restart’ after the model validation gives an iterative scheme.

### 2.5.1 Mathematical Models

Models and/or systems can be roughly divided into classes such as linear and non-linear time invariant or time varying discrete time or continuous time with lumped or with distributed parameters etc. While at first sight the class of linear time invariant models with lumped parameters seems to be rather restricted it turns out in practice that many real life input output behaviors of practical industrial processes can be approximated very well by such a model.

Mathematical models of dynamical systems are used for analysis simulation prediction optimization monitoring fault detection training and control. There are several approaches to generate a model of a system. One could for instance start from first principles such as writing down the basic physical or chemical laws that generate the behavior of the system. This so called white box approach works for simple examples but its complexity increases rapidly for real world systems. In some cases the systems equations are known up to within some unknown parameters, which are estimated using some parameter estimation method gray-box modeling.

Another approach is provided by system identification in which first measurements or observations are collected from the system which are then modeled using

a so-called black-box identification approach. Such an approach basically consists of first defining a parameterization of the model, and then determining the model parameters in such a way that the measurements are explained as accurately as possible by the model. Typically, this is done by formulating the identification problem as an optimization problem in which the variables are the unknown parameters of the model the constraints are the model equations and the objective function a measure of the deviation between the observations and the predictions or simulations obtained from the model.

The field of linear system identification is certainly not new although we can safely say that it only started to blossom in the 1970s. Yet, 20-years of research have generated a lot of results and practical hands on experience. Among the key references of identification are [6, 20, 31, 49].

In what follows, we use data for industrial evaporator from [27].

### 2.5.2 Multistage Evaporator System

The selected evaporator system is the first step in the liquor burning process associated with the Bayer process for alumina production at the Wager up alumina refinery in western Australia. It consists of one falling film, three forced-circulation and a super-concentration evaporators in series [44].

The main components of each stage are a flash tank (FT), a flash pot and a heater (HT). A simplified schematic of the evaporator system is depicted in Fig. 2.7. Flash pots are not shown in this figure for simplicity of the schematic. Spent liquor, which is recovered after precipitation of the alumina from its solution, is fed to the

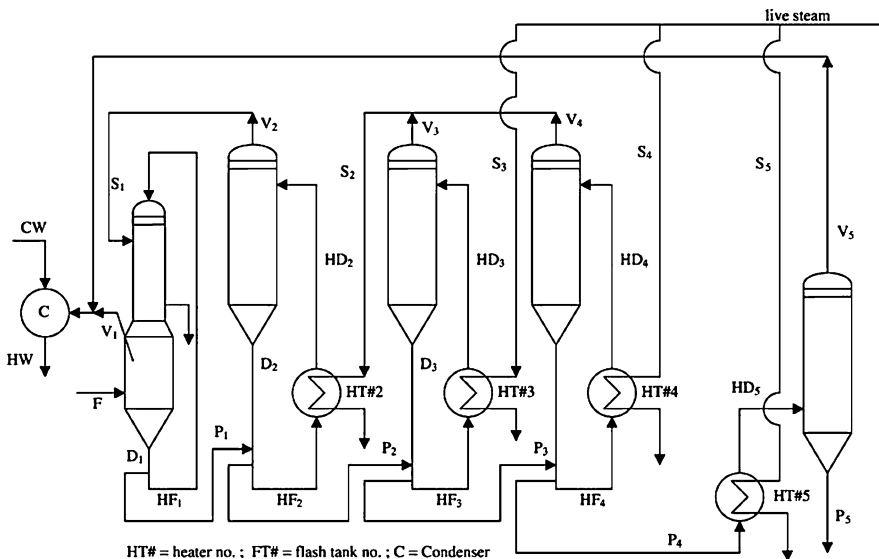


Fig. 2.7 A simplified schematic of the evaporator system

falling film stage (FT #1). The volatile component, water in this case, is removed under high recycle rate and the product is further concentrated through the three forced-circulation stages (FT #2–4). The super-concentration stage (FT #5) is used to remove the residual ‘flashing’ of the concentrated liquor without recycle. In each of the forced-circulation and super-concentration stages, the spent liquor is heated through a shell and tube heat exchanger (heater) and water is removed as vapor at lower pressure in the FT. The vapor given off is used as the heating medium in the heaters upstream. The flashed vapor from FT #3 and 4 are combined and used in HT #2 while the vapor from FT #2 is used in HT #1. The flashed vapor from FT #5 is sent directly to the condenser, *C* in Fig. 2.6. The steam condensates from the heaters are collected in the flash pots. Live steam is used as the heating medium for HT #3, 4 and 5. Live steam to HT #3 is set in ratio to the amount of live steam entering HT #4, while the amount of live steam to HT #5 is set depending on the amount of residual ‘flashing’ to be removed. The cooling water flow to the contact condenser, *C* is set such that all remaining flashed vapor is condensed. The evaporator system is crucial in the aluminum refinery operation and is difficult to control due to recycle streams, strong process interactions and nonlinearities.

## 2.6 Distillation Tower

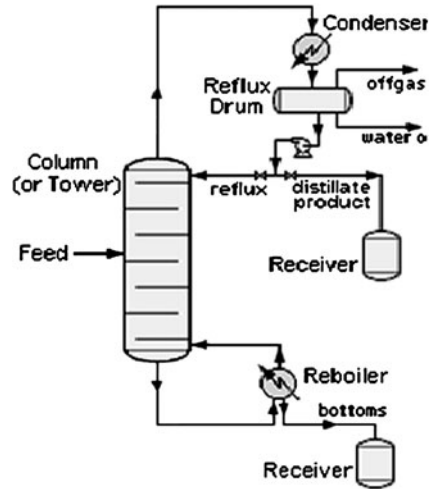
Distillation towers are widely used in the chemical process industries where large quantities of liquids have to be distilled. Industrial distillation towers are usually operated at a continuous steady state. From a practical viewpoint, the most important manipulated variables are the bottom supply energy, the top energy removal, the reflux ratio, which influence the tower operating pressure, the tray load and degree of separation. Concerning the system outputs, a distinction must be made between the controlled and the uncontrolled variables. If the underlying task is to produce a required product quality, then the top and bottom qualities are the most important controlled variables. At a tray only the temperature can be continuously measured and this yields a good indication of the condition of the tower.

There are several assumptions that are commonly made in order not to complicate matters unnecessarily. These assumptions include that the vapor mass at a tray is negligible compared to the liquid mass and the energy content of the vapor mass at a tray is neglected.

### 2.6.1 A Particular Tower

In this section, we focus our study on a class of distillation towers commonly used in natural gas plants, an example of which is in *Aramco-Saudi Arabia*. It must be noted for this class that unless disturbed by changes in feed, heat, ambient temperature, or condensing, the amount of feed being added normally equals the amount of product being removed. A typical physical layout of distillation tower (DT) is portrayed in Fig. 2.8.

Fig. 2.8 Distillation unit



For simplicity in exposition, the identification studies carried out in the subsequent chapter are based on one input and one output data set each of 10080 samples with a sampling period of 60 s:

- Input: Feed inlet temperature in  $F^\circ$ .
- Output: Tower outlet compound of  $C_2$  in mol %.

## 2.7 Falling Film Evaporator

The most common used evaporator in the dairy industry is the falling film evaporator, for the concentration of products like milk, skimmed milk and whey. A four stage evaporator is used to reduce the water content of the product, that is, milk. The data was taken from [21]. The identification scheme used for the data is the N4SID subspace based identification. The data consists of 6305 samples with three inputs, feed flow, vapor flow to the first evaporator stage and cooling water flow and three outputs, dry matter content, the flow and the temperature of the out coming product.

The solution containing the desired product is fed to the evaporator and passes a heat source. The applied heat converts the water in the solution to vapor. The vapor is removed from the rest of the solution and is condensed while the now concentrated solution is either fed into the second evaporator is removed. The evaporator generally as a machine consists of four sections. The heating section consists of the heating medium. Steam is fed into this section. The concentrating and separating section removes the vapor being produced from the solution. The condenser condenses the separated vapor, then the vacuum or pump provides pressure to increase the circulation.

Evaporation is used basically in the dairy industry for the concentration of products like milk, skimmed milk etc. Concentration involves the removal of water from

the product. To minimize the cost, evaporation is usually performed in multiple effect evaporators where two or more effects operate at progressively lower boiling points. In this type of arrangement, the vapor produced in the previous effect can be used as the heating medium in the next. The evaporator considered here is a four falling film effects and has a water evaporation capacity of 800 kg/h. The evaporators most commonly are used in the split effect mode, where only the third effect and the finishing effect are used.

### 2.7.1 A Single Effect Evaporator

In what follows, for simplicity, we will consider a single effect falling film evaporator to outline the operating principles.

A single effect evaporator consists of a balance tank, a condenser, a preheater, an evaporator calandria, a separator and a vacuum pump, see Fig. 2.9. The process can

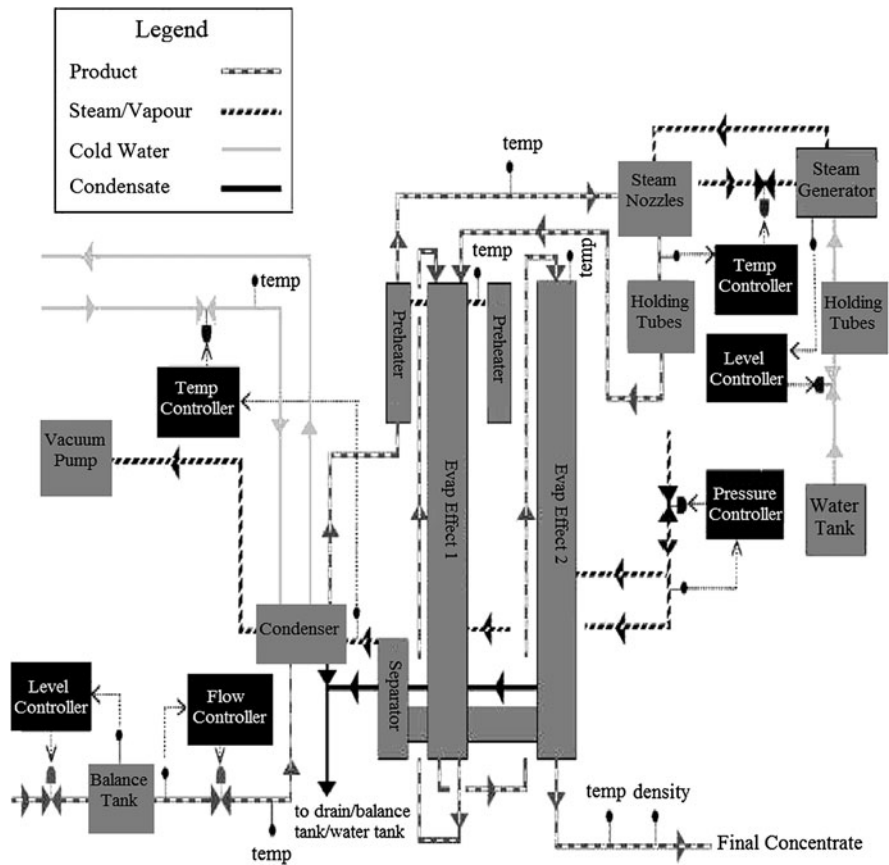
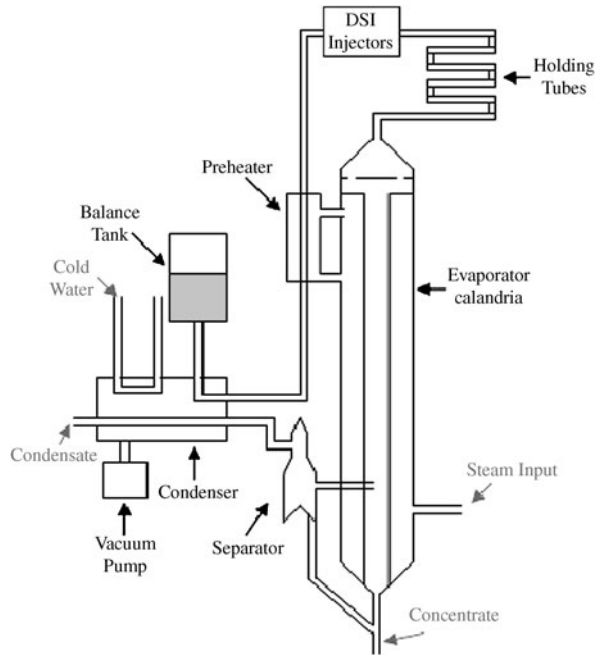


Fig. 2.9 Schematic diagram of evaporator in split effect

**Fig. 2.10** Block diagram of single effect falling film evaporator



be decomposed into a product route (steps **Pa–Pf**), a steam route (steps **Sa–Sc**) and a product vapor route (steps **Va–Vd**). Firstly, we will consider the path the product takes through the evaporator, see Fig. 2.10.

- Pa** From the balance tank, the concentrate flows through the condenser where it gets its first injection of heat—see (**Vc**) overleaf.
- Pb** The product then flows through the preheater where it gets a second injection of heat (see **Sc**).
- Pc** The product is then pasteurized via the Direct Steam Injection (DSI) pasteurization unit and passes through the holding tubes.
- Pd** From the DSI, the product enters the evaporator calandria. A nozzle and spreader plate form a distribution system at the top of the evaporator that ensures a uniform product distribution.
- Pe** Upon leaving the distribution plate, the product flows through stainless steel tubes. The product forms a thin film on the inside of the tube while the outside of the tube is surrounded by steam.
- Pf** The product from the tubes reaches the bottom of the calandria where it is collected along with product from the separator (see **Va**).

Next, consider the steam’s path through the process, see Fig. 2.11.

- Sa** Typically, but not always, the steam enters the calandria at the bottom and surrounds the tubes through which the product is flowing.
- Sb** Heat is then transferred from the steam to the product. This transfer of heat causes the water in the product to boil and produce vapor inside the tubes.

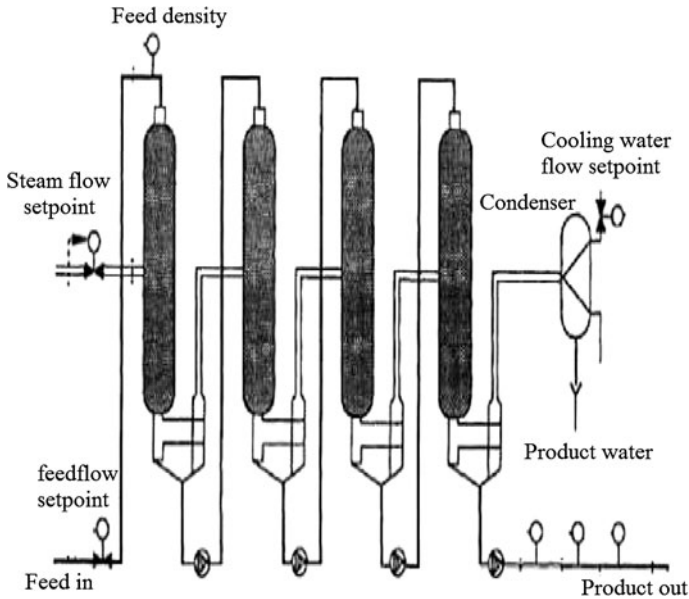


**Fig. 2.11** Four-effect falling film evaporator

**Sc** Some steam from the calandria shell enters the preheater and is used as the heating medium in the preheater (see **Pb**).

Finally, consider the route of the product vapor through the process.

**Va** The product vapor exits the bottom of the calandria and enters the separator where product is removed from the vapor and returned to the product stream.

**Vb** The vapor then enters the condenser.

**Vc** In the condenser, the vapor acts as a heating medium for the product (see **Pa**).

**Vd** The vapor then passes the cold water pipes and condenses.

## 2.8 Vapor Compression Cycle Systems

In vapor compression cycle systems, it is desirable to effectively control the thermodynamic cycle by controlling the thermodynamic states of the refrigerant. By controlling the thermodynamic states with an inner loop, supervisory algorithms can manage critical functions and objectives such as maintaining superheat and maximizing the coefficient of performance.

The primary goal of any air-conditioning or refrigeration system is to move energy from one location to another. An idealized vapor compression cycle (VCC) system, as shown in Fig. 2.12, is a thermodynamic system driven by the phase characteristics of the refrigerant that is flowing through it. Therefore, it is useful to describe the system in terms of the state of its refrigerant, as shown on a pressure-enthalpy ( $P-H$ ) diagram, see Fig. 2.13.

**Fig. 2.12** Schematic diagram of VCC system

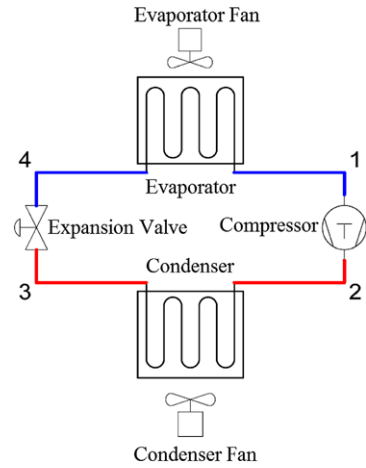
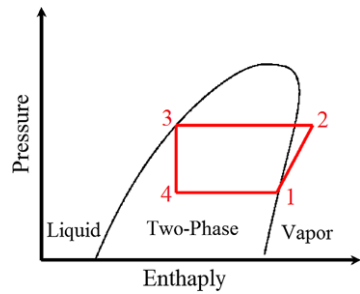


**Fig. 2.13**  $P-H$  cycle diagram

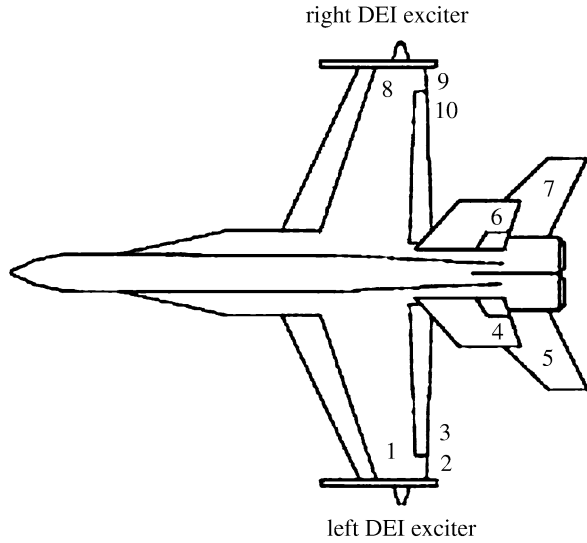


### 2.8.1 A Typical System

An ideal VCC system assumes isentropic compression, isenthalpic expansion, and isobaric condensation and evaporation. The basic control objectives of a VCC system can be conceptualized visually via Fig. 2.13. For example, the difference between  $h_1$  and  $h_4$  represents the increase in enthalpy across the evaporator, that is, the amount of energy removed from the cooled space. This is a measure of evaporator capacity. The difference between  $h_2$  and  $h_1$  represents the increase in enthalpy across the compressor, that is, the amount of work done by the compressor to increase the pressure of the refrigerant vapor. The system coefficient of performance (COP), a measure of system efficiency, is defined as the ratio between these two changes in enthalpy.

The focus of this study is to present a comprehensive controller design approach, that is, one that covers displacement and velocity control, addresses the nonlinearities present in the vapor compression system and considers practical issues such as transient response and real-time implementation.

**Fig. 2.14** F-18 sensor configuration



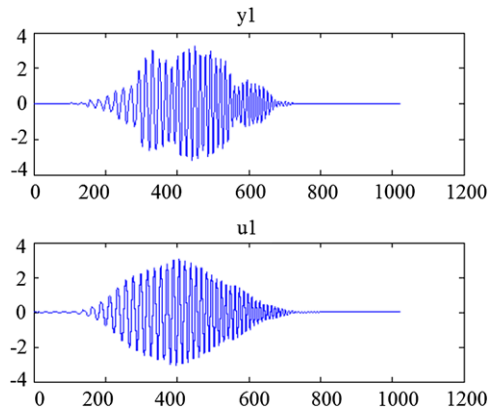
## 2.9 Flutter of an Aircraft F-18

The Flutter is a self-feeding and potentially destructive vibration where aerodynamic forces on an object couple with a structure's natural mode of vibration to produce rapid periodic motion [14]. Flutter can occur in any object within a strong fluid flow, under the conditions that a positive feedback occurs between the structure's natural vibration and the aerodynamic forces, see Fig. 2.14. That is, that the vibration movement of the object increases an aerodynamic loads which in turn drives the object to move further [17, 34]. If the energy during the period of aerodynamic excitation is larger than the natural damping of the system, the level of vibration will increase, resulting in self-exciting oscillation. The vibration levels can thus build up and are only limited when the aerodynamic or mechanical damping of the object match the energy input, this often results in large amplitudes and can lead to rapid failure. Because of this, structures exposed to aerodynamic forces—including wings, aerofoil, but also chimneys and bridges—are designed carefully within known parameters to avoid flutter. It is however not always a destructive force; recent progress has been made in small-scale wind generators for underserved communities in developing countries, designed specifically to take advantage of this effect.

### 2.9.1 Flutter Input and Output Data

The data comprises of one input and one output which has a sampling time of 1 s, the number of samples in the data are 1024, see Fig. 2.15. In this section, the data is subdivided into the *estimation* and *validation* data parts, each part is comprised

**Fig. 2.15** Flutter input and output data



of 512 samples. As we shall see in later chapters, applications of the identification techniques are employed on the estimation data and then the estimated models are evaluated on the validation data.

## 2.10 A Hydraulic Pumping System

It is often desirable to find parsimonious models with good static and dynamical responses [32]. The estimation of nonlinear models with such features is quite hard mainly because static and dynamic information are not equally weighed in a single set of data. In this respect, static and dynamic information can be thought of as being conflicting. Flexible black-box structures are able to accurately fit a single piece of data. However, there are two main drawbacks with most of such structures. First, once such models are estimated, the static information (e.g., static nonlinearity) is not readily available analytically. Second, not all such model structures and algorithms have been adapted to permit the effective use of static information during training (parameter estimation). It should be noticed that black-box identification does not necessarily guarantee correct steady-state performance when the model is nonlinear [3].

When the data sets are conflicting in some way, it is advisable to use multi-objective approaches which yield a set of optimal solutions called the Pareto set. Bi-objective algorithms have proved to be quite useful in combining both static and dynamic data during model identification [10].

In what follows, we aim to identify models of a 15 kW hydraulic pumping system. There has been a clear increase of variable frequency drives as the final control element for such systems. This has enabled the implementation of fast and automatic control systems. Models of such systems are highly desirable for characterization and control. Such models should, ideally, represent the system accurately both in transient and steady-state regimes over a wide range of operating conditions. This requires, more often than not, the use of nonlinear models.

We focus in this book to obtain models that perform well both in transient and steady-state regimes, different identification approaches were implemented to “guarantee” a good balance between such features. In order to improve the model steady-state performance, the measured static curve of the pumping system was used as auxiliary information. Such information was used in different intensities, depending on the model representation used. An improved bi-objective identification approach is presented and a new decision-maker is defined. In this brief, we used and compared polynomial and neural nonlinear autoregressive with moving average and exogenous variables (NARMAX) models.

### 2.10.1 Hydraulic Process and the Data

In a full-scale hydroelectric power plant (over 80% of Brazilian electrical energy is produced in such plants), the water head can be considered constant over reasonably long periods of time. At testing plants, however, the turbines are fed by powerful hydraulic systems and not by a water head. Because of the characteristics of the centrifugal pumps used in such plants, the pressure on the turbine decreases as the water flow increases. Therefore, in realistic testing plants, pressure must be controlled over a wide range of operating conditions. Mathematical models are desired to simulate and to design the closed-loop control of the real pumping system, where the models output is the system pressure and the models input is the pumps reference speed.

The hydraulic plant described in this section is composed by two centrifugal pumps that feed a hydraulic turbine. The hydraulic plant should be seen by the turbine as a water head. The static and dynamic data used in this brief were measured from this plant, composed by two centrifugal pumps coupled to induction motors of 7.5 kW and variable speed drive systems (see Fig. 2.16). The pumps can be operated alone, in parallel or in a series configuration, always at the same speed. In this work, the pumps were set in a parallel configuration working at the same instantaneous speed with a Francis turbine as load [9].

**Fig. 2.16** Hydraulic pumping system

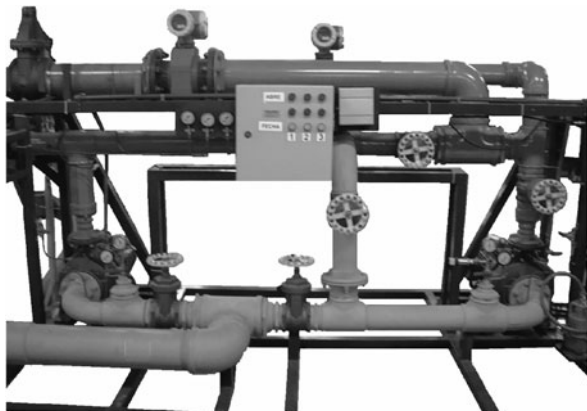
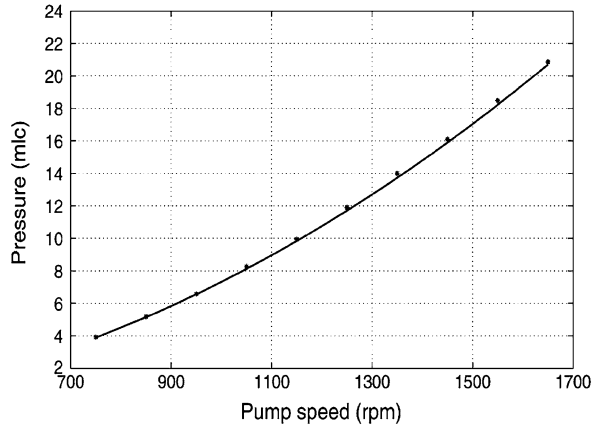


**Fig. 2.17** Static curve of the hydraulic pumping system and its approximation



The modeling data presented in this work were collected from a data acquisition system. The piezo-resistive pressure transmitter error is  $\pm 0.175$  mlc (meter of liquid column).

### 2.10.2 Static Behavior

The static curve of the system was measured by:

1. Setting the turbine distributor blade to 50% and
2. Maintaining the pumps speed fixed at the chosen values—the speed references of both pumps were maintained the same during this procedure. After transients died out, the output pressure was recorded for each reference speed.

During this test, the pumps speed was varied from 750 to 1650 r/min. The static curve is shown in Fig. 2.17 as well as the second-order polynomial approximation

$$H(\bar{u}) = \beta \bar{u}^2 + \alpha \bar{u} + \kappa \quad (2.5)$$

with  $\beta = 7.2652 \times 10^{-6}$ ,  $\alpha = 1.4933 \times 10^{-3}$ ,  $\kappa = -1.3312$ , and where is the pressure in the output pipe and is the steady-state pump speed. This static curve will be useful during the gray-box modeling and will also be used to evaluate the identified models.

In Chap. 4, we will perform identification methods to generate appropriate models.

## 2.11 Notes and References

In this introductory chapter, some representative system applications were presented to help in motivating the readers to the upcoming topics. It must be emphasized that the target goal is to launch an information-based approach to control system design.

Being an applied design approach, we start by examining some industrial systems and shed light into their input/output variables. Indeed, there are many similar systems in practice and hence we encourage the readers to look at these systems and apply the methods of this book. We will make every effort to produce the subsequent chapters as a self-contained examination of the background and methods of industrial dynamical systems. For a good introduction to the subject matter, the reader is referred to [1, 2, 4, 5, 7, 8, 11–13, 15–19, 22, 23, 28, 29, 33–41]. For a MATLAB tool box, it is advisable to consult [40, 42, 43].

## References

1. Abdelazim, T., Malik, O.: Identification of nonlinear systems by Takagi–Sugeno fuzzy logic grey box modeling for real-time control. *Control Eng. Pract.* **13**(12), 1489–1498 (2005)
2. Aguirre, L.A.: A nonlinear correlation function for selecting the delay time in dynamical reconstructions. *Phys. Lett.* **203A**(2–3), 88–94 (1995)
3. Aguirre, L.A., Donoso-Garcia, P.F., Santos-Filho, R.: Use of a priori information in the identification of global nonlinear models—A case study using a buck converter. *IEEE Trans. Circuits Syst. I, Regul. Pap.* **47**(7), 1081–1085 (2000)
4. Aguirre, L.A., Barroso, M.F.S., Saldanha, R.R., Mendes, E.M.A.M.: Imposing steady-state performance on identified nonlinear polynomial models by means of constrained parameter estimation. *IEE Proc. Part D. Control Theory Appl.* **151**(2), 174–179 (2004)
5. Aguirre, L.A., Coelho, M.C.S., Corrêa, M.V.: On the interpretation and practice of dynamical differences between Hammerstein and Wiener models. *IEE Proc. Part D. Control Theory Appl.* **152**(4), 349–356 (2005)
6. Astrom, K.J., Eykhoff, P.: System identification—A survey. *Automatica* **7**(2), 123–162 (1971)
7. Baker, J.E.: Reducing bias and inefficiency in the selection algorithm. In: *Proc. 2nd Int. Conf. Genetic Algorithms Genetic Algorithms Their Appl.*, Mahwah, N.J., pp. 14–21 (1987)
8. Bakker, H.H.C., Marsh, C., Paramalingam, S., Chen, H.: Cascade controller design for concentration in a falling film evaporators. *Food Control* **17**(5), 325–330 (2006)
9. Barbosa, B.H.: Instrumentation, modelling, control and supervision of a hydraulic pumping system and turbine-generator module (in Portuguese). Master's thesis, Sch. Elect. Eng., Federal Univ. Minas Gerais, Belo Horizonte, Brazil (2006)
10. Barroso, M.S.F., Takahashi, R.H.C., Aguirre, L.A.: Multi-objective parameter estimation via minimal correlation criterion. *J. Process Control* **17**(4), 321–332 (2007)
11. Billings, S.A., Voon, W.S.F.: Least squares parameter estimation algorithms for nonlinear systems. *Int. J. Syst. Sci.* **15**(6), 601–615 (1984)
12. Billings, S.A., Chen, S., Korenberg, M.J.: Identification of MIMO nonlinear systems using a forward-regression orthogonal estimator. *Int. J. Control* **49**(6), 2157–2189 (1989)
13. Bingulac, S., Sinha, N.K.: On the identification of continuous-time systems from the samples of input–output data. In: *Proc. Seventh Int. Conf. on Mathematical and Computer Modeling*, Chicago, IL, pp. 231–239 (1989)
14. Buchares, A., Cassan, H., Roubertier, J.: Advanced parameter identification techniques for near real-time flight flutter test analysis. *AIAA*, Paper 90-1275, May 1990
15. Chen, S., Billings, S.A., Luo, W.: Orthogonal least squares methods and their application to nonlinear system identification. *Int. J. Control* **50**(5), 1873–1896 (1989)
16. Connally, P., Li, K., Irwing, G.W.: Prediction and simulation error based perceptron training: Solution space analysis and a novel combined training scheme. *Neurocomputing* **70**, 819–827 (2007)
17. Cooper, J.: Parameter estimation methods for the flight flutter testing. In: *Proc. the 80th AGARD Structures and Materials Panel, CP-566, AGARD, Rotterdam, The Netherlands* (1995)

18. Correa, M.V., Aguirre, L.A., Saldanha, R.R.: Using steady-state prior knowledge to constrain parameter estimates in nonlinear system identification. *IEEE Trans. Circuits Syst. I, Regul. Pap.* **49**(9), 1376–1381 (2002)
19. Cunningham, P., Canty, N., O'Mahony, T., O'Connor, B., O'Callaghan, D.: System identification of a falling film evaporator in the dairy industry. In: *Proc. of SYSID'94, Copenhagen, Denmark*, vol. 1, pp. 234–239 (1994)
20. De Moor, B.L.R. (ed.): *DaISy: Database for the Identification of Systems*. Department of Electrical Engineering, ESAT/SISTA, K.U.Leuven, Belgium. <http://www.esat.kuleuven.ac.be/sista/daisy>
21. De Moor, B.L.R., Ljung, L., Zhu, Y., Van Overschee, P.: Comparison of three classes of identification methods. In: *Proc. of SYSID'94, Copenhagen, Denmark*, vol. 1, 175–180 (1994)
22. Draper, N.R., Smith, H.: *Applied Regression Analysis*, 3rd edn. Wiley, New York (1998)
23. Ekawati, E., Bahri, P.A.: Controllability analysis of a five effects evaporator system. In: *Proc. Foundations of Computer-Aided Process Operations, FOCAP02003*, pp. 417–420 (2003)
24. El-Sherief, H., Sinha, N.K.: Identification and modelling for linear multivariable discrete-time systems: A survey. *J. Cybern.* **9**, 43–71 (1979)
25. El-Sherief, H., Sinha, N.K.: Determination of the structure of a canonical model for the identification of linear multivariable systems. *IEEE Trans. Syst. Man Cybern.* **SMC-12**, 668–673 (1982)
26. Energy Efficiency and Renewable Energy, U.S. Department of Energy. [www.energy.gov](http://www.energy.gov)
27. Favoreel, W., De Moor, B.L.R., Van Overschee, P.: Subspace state-space system identification for industrial processes. *J. Process Control* **10**(2–3), 149–155 (2000)
28. Ghiaus, C., Chicinas, A., Inard, C.: Grey-box identification of air-handling unit elements. *Control Eng. Pract.* **15**(4), 421–433 (2007)
29. Goldberg, D.E.: *Genetic Algorithms in Search, Optimization and Machine Learning*. Addison-Wesley, New York (1989)
30. Hsia, T.C.: On sampled-data approach to parameter identification of continuous-time linear systems. *IEEE Trans. Autom. Control* **AC-17**, 247–249 (1972)
31. Hsia, T.: *System Identification: Least-Squares Methods*. Lexington Books, Lexington (1977)
32. Jakubek, S., Hametner, C., Keuth, N.: Total least squares in fuzzy system identification: An application to an industrial engine. *Eng. Appl. Artif. Intell.* **21**, 1277–1288 (2008)
33. Karimi, M., Jahanmiri, A.: Nonlinear modeling and cascade control design for multieffect falling film evaporator. *Iran. J. Chem. Eng.* **3**(2) (2006)
34. Kehoe, M.W.: A historical overview of flight flutter testing, NASA TR 4720, Oct. 1995
35. Leontaritis, I.J., Billings, S.A.: Input–output parametric models for nonlinear systems. Part II: Deterministic nonlinear system. *Int. J. Control* **41**(2), 329–344 (1985)
36. Miranda, V., Simpson, R.: Modelling and simulation of an industrial multiple-effect evaporator: Tomato concentrate. *J. Food Eng.* **66**, 203–210 (2005)
37. Neilsen, K.M., Pedersen, T.S., Nielsen, J.F.D.: Simulation and control of multieffect evaporator
38. Nepomuceno, E.G., Takahashi, R.H.C., Aguirre, L.A.: Multiobjective parameter estimation: Affine information and least-squares formulation. *Int. J. Control* **80**(6), 863–871 (2007)
39. Norgaard, M.: Neural network based system identification—TOOLBOX, Tech. Univ. Denmark, Lyngby, Tech. Rep. 97-E-851 (1997)
40. Ogata, K.: *MATLAB for Control Engineers*. Prentice-Hall, New York (2008)
41. Pan, Y., Lee, J.H.: Modified subspace identification for long-range prediction model for inferential control. *Control Eng. Pract.* **16**(12), 1487–1500 (2008)
42. Piroddi, L.: Simulation error minimization methods for NARX model identification. *Int. J. Model. Identif. Control* **3**(4), 392–403 (2008)
43. Piroddi, L., Spinelli, W.: An identification algorithm for polynomial NARX-models based on simulation error minimization. *Int. J. Control* **76**(17), 1767–1781 (2003)
44. Rangaiah, G., Saha, P., Tade, M.: Nonlinear model predictive control of an industrial four-stage evaporator system via simulation. *Chem. Eng. J.* **87**, 285–299 (2002)
45. Roffel, B., Betlem, B.: *Process Dynamics and Control*. Wiley, London (2006)

46. Sinha, N.K.: Estimation of transfer function of continuous-time systems from samples of input–output data. *Proc. Inst. Electr. Eng.* **119**, 612–614 (1972)
47. Sinha, N.K., Kuszta, B.: *Modelling and Identification of Dynamic Systems*. Von-Nostrand Reinhold, New York (1983)
48. Sinha, N.K., Rao, G.P. (eds.): *Identification of Continuous-Time Systems*. Kluwer Academic, Dordrecht (1991)
49. Soderstrom, T., Stoica, P.: *System Identification*. Prentice-Hall, New York (1989)